A Range Rate Based Detection Technique for Tracking A Maneuvering Target

Jifeng Ru   Huimin Chen   X. Rong Li
Department of Electrical Engineering
University of New Orleans
New Orleans, LA 70148
Phone: 504-280-1280
Email: {jru,hchen2,xli}@uno.edu

Genshe Chen
Intelligent Automation, Inc.
15400 Calhoun Dr. Suite 400
Rockville, MD 20855
Phone: 301-294-5218
gchen@i-a-i.com

ABSTRACT

In this paper a novel approach for detecting unknown target maneuver using range rate information is proposed based on the generalized Page's test with the estimated target acceleration magnitude. Due to the high nonlinearity between the range rate measurement and the target state, a measurement conversion technique is used to treat range rate as a linear measurement in Cartesian coordinates so that a standard Kalman filter can be applied. The detection performance of the proposed algorithm is compared with that of existing maneuver detectors over various target maneuver motions. In addition, a model switching tracker based on the proposed maneuver detector is compared with the state-of-the-art IMM estimator. The results indicate the effectiveness of the maneuver detection scheme which simplifies the tracker design. The tracking performance is also evaluated using a steady state analysis.

1. INTRODUCTION

Maneuvering target tracking (MTT) is challenging due to the fact that the target acceleration is generally unknown and not directly available through radar measurements. Decision based techniques for MTT have been studied extensively in the literature, where the target state estimation is based on a motion model determined by the maneuver detector. Clearly, reliable and timely decision on the target maneuver onset time is the key to this approach. There exist quite a few algorithms to detect unknown target maneuvers.[17, 22] These algorithms usually rely on the linear Gaussian assumption of the target dynamic model and measurement equation. In addition, some approaches make soft decisions between non-maneuver and maneuver target motions, as in multiple model estimation.[2]

Recently, a range rate (also known as the radial or Doppler velocity) based target maneuver detection has been proposed.[6] The results indicate that the use of range rate information helps detect target maneuvers and estimate the maneuver magnitude by assuming a constant turn rate motion. It is believed that the maneuver detection performance relies heavily on the accuracy of the range rate measurement as well as the maneuver model. Similar research efforts have been made to improve the maneuvering target tracking performance by exploiting the range rate information.[8–12, 27] Since range rate measurements are highly nonlinear with respect to the target state in the Cartesian coordinates, conventional methods either convert target position and radial velocity measurements from the polar to the Cartesian coordinates or apply the extended Kalman filter (EKF) of various kinds, which sometimes may diverge due to large linearization error. The error compensation methods of measurement conversion from the polar to the Cartesian coordinates were studied based on linearization or nested conditioning.[3, 11, 28] Several sequential filters were proposed to process position and range rate measurements.[9, 10] However, those techniques still rely on the EKF to incorporate the range rate measurement.

This paper intends to address the following issue: how to effectively incorporate range rate information for maneuver detection and tracking when a Kalman filter based tracker is used.

First, based on our previous study,[23] incorporation of range rate measurements in the Kalman filter based tracker design is a nontrivial issue. We propose a measurement conversion technique to treat range rate as a linear measurement in the Cartesian coordinates so that the standard Kalman filter can be directly applied.[1]

Second, we refine the maneuver magnitude estimate that indicates the total acceleration along both tangential and normal directions rather than the minimum *turn* acceleration estimate in reference.[6] We further investigate the maneuver detector based on Page's test, which is also known as cumulative sums (CUSUM) test.[13,14,21] It yields the quickest maneuver detection if the target maneuver motion is known while the only unknown quantity is the maneuver onset time. The major challenge of this approach is to find a reliable test statistic that can distinguish between non-maneuver and maneuver motions. We use Gamma distribution to approximate the empirical probability density function (pdf) of the estimated total target acceleration. Based on the approximated pdf, the generalized Page's test can be developed for different target maneuver motions with various approximate Gamma distributions.

Third, we are interested in the performance improvement using range rate information by comparing the proposed maneuver detector with several renowned maneuver detection algorithms, including measurement residual based detector[17] and minimum turn acceleration based detector.[6] We also want to compare the model switching tracker using our maneuver detection method with the interacting multiple model (IMM) estimator,[17] which does not make a hard decision on whether the target is maneuvering or not.

Another important issue is the performance comparison in terms of estimation accuracy when range rate information is either used or ignored by the tracker. We simplify the analysis by using the steady state estimation error of a Kalman filter to indicate the ideal error bounds with and without range rate measurements. The results help understand the tracking performance obtained with realistic target maneuvers and serve as a guideline for the tracker design where performance degradation is expected due to the uncertainty of target maneuver capability.

The rest of the paper is organized as follows. Section 2 formulates the target maneuver detection and tracking problem. Section 3 presents different maneuvering detection algorithms including the proposed Page's test based on the estimated total acceleration. A measurement conversion technique is also presented to treat the range rate as a linear measurement of the target state. Section 4 discusses the tracker design issues for the model switching tracker and the multiple model estimator. Section 5 evaluates the detection and estimation performance using realistic E2C tracking scenarios[25,26] with various target maneuver motions along tangential and normal directions. Section 6 presents the comparison of tracking accuracy with and without range rate information based on a steady state analysis. Section 7 summarizes the results and discusses a few future research tasks.

2. PROBLEM FORMULATION

2.1. Target Dynamic Model and Measurement Equation

Without loss of generality, we consider a target motion being modeled in the two-dimensional Cartesian coordinates given by[4]

$$x_{k+1} = Fx_k + Gw_k \tag{1}$$

where the state includes the position and velocity along x and y axes; the process noise is a zero-mean white Gaussian acceleration sequence $w_k \sim \mathcal{N}(0, Q_k)$; the time invariant matrices are $G = \text{diag}[G_2, G_2]$ and $F = \text{diag}[F_2, F_2]$ where

$$G_2 = \begin{bmatrix} \frac{1}{2}T^2 \\ T \end{bmatrix} \quad F_2 = \begin{bmatrix} 1 & T \\ 0 & 1 \end{bmatrix}$$

and T is the sampling time. The effect of target maneuver is modeled by a large process noise.

We assume that the radar is fixed at the origin. The measurement equation can be written as

$$z_k = h(x_k) + v_k \tag{2}$$

where $z_k = [\ r_k \quad \theta_k \quad \dot{r}_k\ ]'$ contains the range, bearing and range rate measurement; v_k is the corresponding measurement noise vector with Gaussian distribution given by $v_k \sim \mathcal{N}(0, R_k)$. We drop the time index k in the sequel if it does not cause any confusion. The measurement equations for target range, bearing and range rate are give by $r = \sqrt{x^2 + y^2} + v_r$, $\theta = \text{tg}^{-1}(y/x) + v_\theta$, $\dot{r} = \frac{x\dot{x} + y\dot{y}}{\sqrt{x^2+y^2}} + v_{\dot{r}}$, respectively.

2.2. Formulation of Maneuver Detection Problem

We assume that the non-maneuver target motion is modeled by nearly constant velocity with known process noise power spectral density (PSD).[4] If a target starts a maneuver with unknown acceleration magnitude a at an unknown time n, the maneuver onset detection problem can be formulated as testing the following two hypotheses:

H_0 : target is not maneuvering, $a_m = 0$ for all $m = 1, ..., k$;

H_1 : target starts a maneuver at an unknown time n, $a_m \neq 0$ for some $m = n, ..., k$.

This problem is also known as the change point detection in the statistics literature,[5] where the hypothesis H_1 is composite due to the unknown parameters a and n.

3. MANEUVER DETECTION WITH RANGE RATE MEASUREMENTS

Existing maneuver detection algorithms can be classified into two types of hypothesis tests: chi-square based test, which does not require the knowledge of target maneuver and likelihood ratio based test, which does. A more detailed performance comparison of maneuver detection methods can be found in.[17,22,24] Most maneuver detection algorithms rely on the assumption that the residual sequence of the filter is white Gaussian. Notice that the range rate measurement can be a direct indicator of possible target maneuver even when the residue sequence deviates from Gaussian distribution, we want to exploit its proper usage for quick detection of target maneuvers.

3.1. Total Target Acceleration Based Detector

Since a range rate measurement itself can be quite noisy, an estimation technique is required to obtain the magnitude of the target acceleration. A novel approach was developed[6] to model nearly constant turn rate target maneuvers. Specifically, at time k, the target speed is estimated by $s_k = s_{k-1} = \sqrt{\hat{\dot{x}}_{k-1} + \hat{\dot{y}}_{k-1}}$. The target heading is estimated by $\alpha_{k-1} = \tan^{-1}(\frac{\hat{\dot{x}}_{k-1}}{\hat{\dot{y}}_{k-1}})$; the angular difference between the inverse bearing and the target heading is estimated by $\gamma_k = \cos^{-1}(-\frac{\dot{r}_k}{s_k})$. The two possible target headings are $\alpha_k = (\theta_k + \pi) \pm \gamma_k$ with the target bearing being estimated by $\theta_k = \tan^{-1}(\frac{\hat{x}_{k-1}}{\hat{y}_{k-1}})$. The minimum heading change of the target is given by $\tau_{\min} = \min\{(\alpha_k - \alpha_{k-1}) \bmod 2\pi, (\alpha_{k-1} - \alpha_k) \bmod 2\pi\}$. Thus the minimum target turn acceleration is

$$c_{\min} = \frac{s_k \tau_{\min}}{T} \tag{3}$$

where T is the sampling interval. Note that the distribution of the test statistic under the non-maneuver hypothesis H_0 is difficult to obtain. We found that the tail distribution of $c_{\min}$ under H_0 becomes heavier as the process noise or the measurement error covariance increases.

Since the $c_{\min}$ detector only estimates the target turn acceleration which is sensitive to radar-target geometry, it is natural to use the total acceleration along both tangential and normal directions as target maneuver indicator. At time k, the tangential acceleration is estimated by

$$\hat{a}_t = \frac{\left| \hat{\dot{x}}_{k-1} \sin\theta_k + \hat{\dot{y}}_{k-1} \cos\theta_k - \dot{r}_k \right|}{|\cos\gamma_k|\, T} \tag{4}$$

The normal acceleration is estimated by $\hat{a}_n = c_{\min}$. The total target acceleration is thus given by

$$\hat{a} = c_{\min 2} = \sqrt{\hat{a}_t^2 + \hat{a}_n^2} \tag{5}$$

The detector is denoted as $c_{\min 2}$. The major issue for the above two acceleration based detectors is threshold selection for a desired test size since the distribution of the test statistic under H_0 does not have a closed form.

As observed in our previous study,[23] by including the range rate measurement in the Kalman filter update, the tracker becomes less credible when process noise PSD is small. An alternative is to exploit the range rate information in the maneuver detection only. The Kalman filter updates the state estimates only with the range and bearing measurements. This approach is denoted as $c_{\min 3}$.

3.2. Generalized Page's Test Based Detector

Page's test, also known as the cumulative sums (CUSUM) test, guarantees the quickest maneuver detection with a given false alarm rate when the target maneuver motion is known. The test computes the cumulative sum of the log-likelihood ratio between H_1 and H_0.[13, 14, 21] This can be summarized as follows. Denote by $L_k = \log \frac{f(z^k|H_1)}{f(z^k|H_0)}$ the log-likelihood ratio of two hypotheses H_1 and H_0 based on the measurements $z^k \triangleq (z_1, ..., z_k)$ up to time k. Then Page's test is a sequential detection scheme implemented as follows.[5]

$$L_k = \max \left\{ L_{k-1} + \log \frac{f\left(z_k|H_1, z^{\kappa-1}\right)}{f\left(z_k|H_0, z^{\kappa-1}\right)},\ 0 \right\}, \quad L_0 = 0 \tag{6}$$

where $f\left(z_\kappa|H_i, z^{\kappa-1}\right)$ $(i = 0, 1)$ are the marginal likelihood functions of the hypotheses. A target maneuver is declared if $L_k \geq \lambda$; otherwise the test continues. The stopping time $\hat{n} = \min\{k : L_k \geq \lambda\}$ is the time that a target maneuver is declared.

Based on the estimated target acceleration $\hat{a}$ ($c_{\min 2}$ or $c_{\min 3}$), using the range rate measurement, we can obtain the empirical distribution of the target acceleration statistic in both non-maneuver and maneuver cases. Since Gamma density is flexible to approximate the distribution of the estimated total acceleration when it is not multi-modal, we assume

$$f(\hat{a}|\beta, \gamma) = \frac{1}{\gamma^\beta \Gamma(\beta)} \hat{a}^{\beta-1} e^{-\frac{\hat{a}}{\gamma}} \tag{7}$$

where β and γ are the parameters depending on the underlying hypothesis and $\Gamma(\beta) = \int_0^\infty e^{-t} t^{\beta-1} dt$ is the standard Gamma function. We use maximum likelihood estimates (MLEs) $\hat{\beta}$ and $\hat{\gamma}$ obtained through simulated target motions. These empirical distributions are obtained off-line with a class of target maneuver motions where a Kalman filter based tracker is used. Based on the approximated density $f(\hat{a}|\hat{\beta}, \hat{\gamma})$ under each hypothesis, we can formulate maneuver detection problem as follows

H_0: non-maneuver with a known distribution of total acceleration $f_0(\hat{a}|\hat{\beta}, \hat{\gamma})$

H_1: target starts to maneuver at time n in one of the K possible motions corresponding to the distribution of the total acceleration $f_i(\hat{a}|\hat{\beta}, \hat{\gamma})$, $i = 1, ...K$.

Note that H_1 is a composite hypothesis including multiple possible distributions, each of which corresponds to a particular maneuver motion indicated by the estimated acceleration. Specifically, $f_i(\hat{a})$ may belong to different distribution family with certain unknown parameters.

One way to implement the above scheme is to run K Page's detectors in parallel with various thresholds based on the desired false alarm rate for each target maneuver type. The test has the form

$$L_k^j = \max \left\{ 0, L_{k-1}^j + \frac{\log f_j(\hat{a})}{\log f_0(\hat{a})} \right\}, j = 1, ...K \tag{8}$$

with $L_0^j = 0$. We denote this test as a generalized Page's test since the threshold for L_k^j corresponds to the j-th target maneuver model (in terms of the acceleration magnitude) being true. A model switching tracker can be designed accordingly. Clearly, in order to properly employ this scheme for tracking, the model set design for multiple model trackers is of great importance, i.e., how to choose maneuver models to cover the target motion space in a cost-effective way. Results in references[15, 20] provide theoretical analysis and practical examples.

3.3. Range Rate Measurement Conversion

In the previous discussion, we assume that a Kalman filter is used under different target motions. However, tracking in the Cartesian coordinates with polar measurements is a nonlinear estimation problem. Measurement conversion methods have been extensively studied as in[3, 7, 16] and the references therein. The basic idea is to transform the nonlinear measurement equation into a pseudo linear form in the Cartesian coordinates and then estimate the bias and covariance resulted from the converted-measurement error. However, the range rate measurement can not be directly converted into a linear function of the Cartesian velocity vector. A lot of efforts have been made to study the performance of the EKF with different linearization techniques. Among these, a couple of filter divergence instances were reported when using the EKF.[6]

Due to the simplicity of the Kalman filter and the reliance on the Kalman filter output for a set of existing target maneuver detectors, we adopt a simple scheme to convert the range rate into a linear measurement and provide an analytic formula for bias compensation when range rate measurement error is small.[1] Technical details are given in Appendix A. Note that the bias compensation for the range rate measurement is unnecessary whenever the bias significance factor is relatively small. This is the case for the E2C simulation scenarios to be discussed next where one has good range and bearing measurement accuracy.[25, 26] As such, the state estimation can be implemented within a *linear* framework. The above measurement conversion technique enables us to compare the performance of various target maneuver detectors in a standard Kalman filter setting.

4. TRACKER DESIGN

We would like to investigate the performance gain in tracking accuracy by using the range rate measurement. A variety of techniques have been developed for maneuvering target tracking in the literature.[4, 17] One of the widely used techniques in decision-based approach is the noise-level adjustment. It is assumed that the effect of a target maneuver can be accounted for by increasing the process noise level (i.e., the covariance matrix Q). When a maneuver is detected, the Kalman filter will switch from a lower to a higher process noise level. The goal is to achieve good tracking performance under both non-maneuver and maneuver motions. Alternatively, the multiple model (MM) approaches have been extensively studied and demonstrated as a cost effective tool to handle the target motion uncertainty among which the interacting multiple model (IMM) is considered the state-of-the-art tracker.[19] Thus we compare the maneuver detection based model switching tracker with the IMM estimator under different types of target accelerations. The white noise acceleration (WNA) model[4] with two levels is used in the model switching tracker. The low level Q_{low} is for the non-maneuver case while the high level Q_{high} is for the maneuver motion. The two-model IMM tracker has similar design of Q_{low} and Q_{high} for the non-maneuver and maneuver modes, respectively.

5. SIMULATION STUDY

In order to evaluate the maneuver detection performance with and without the range rate information, scenarios representing different aspects of the target motion are generated by a curvilinear model. These scenarios, although simple, characterize the typically encountered maneuver motions of an aircraft.

5.1. Ground Truth Target Trajectory Generation

The continuous time 2D curvilinear motion model is given by[18]

$$\dot{x}(t) = v(t)\cos\phi(t) + w_x(t) \tag{9}$$

$$\dot{y}(t) = v(t)\sin\phi(t) + w_y(t) \tag{10}$$

$$\dot{v}(t) = a_t(t) + w_v(t) \tag{11}$$

$$\dot{\phi}(t) = a_n(t)/v(t) + w_\phi(t) \tag{12}$$

where (x, y), v, ϕ denote the target position, speed and heading. This model is fairly general since it accounts for along- and cross-track accelerations along the tangential and normal directions. Note that by using a curvilinear motion model to generate the ground truth, there is a *model mismatch* between the true target motion and the Kalman filter based on a WNA model with a low or high process noise level. This model mismatch is typical in real tracking and we want to keep the ground truth close to the E2C operational profiles, so the design of the maneuver detector and of the multiple model tracker becomes harder.

5.1.1. Tracking Scenarios

The initial state of the target is (x_0,y_0,v_0,ϕ_0)=(60km, 90km, 412m/s, 45 deg) with small noise disturbance $\sigma_{w_x} = 0.05$m, $\sigma_{w_y} = 0.05$m, $\sigma_{w_v} = 0.025$m/s and $\sigma_{w_\phi} = 0.001$ deg. The radar is located at the origin and measures target range, bearing and range rate. The range measurement noise is a random variable uniformly distributed over ±60 feet. The range rate measurement noise is a random variable uniformly distributed over ±4 knots. The bearing measurement noise is zero mean with standard deviation $\sigma_\theta = 7$mrad. The sampling time $T = 0.25$s. These parameters are chosen in accordance with the typical E2C tracking scenario using an APS-145 radar.[25,26] The following four scenarios are used for performance evaluation with the acronyms highlighted.

(E2C0) Deterministic non-maneuvering scenario. The target moves at a constant velocity during $k = [1, 250]$.

(E2C(a_t, a)) Deterministic tangential acceleration scenario. The target makes a tangential/normal maneuver during $k = [130, 250]$ with a magnitude of a m/s^2.

(E2C(a_n, a)) Deterministic normal acceleration scenario. The target makes a tangential/normal maneuver during $k = [130, 250]$ with a magnitude of a m/s^2.

(E2C(a_n, a)-E2C(a_t, b)) The target makes a normal maneuver during $k = [130, 209]$ with a magnitude of a m/s^2 and tangential acceleration during $k = [210, 300]$ with a magnitude of b m/s^2.

The first scenario is used to demonstrate the filter behavior designed for non-maneuver target motion. The second scenario is designed to examine the average detection delay under different maneuver types and magnitudes. The smaller a is, the harder the maneuver motion is to detect. The last one contains different maneuver motions in two successive maneuvers.

5.2. Performance Measures

The following measures are used to evaluate the performance of the candidate algorithms.

5.2.1. Measures for Detection and Estimation Accuracy

The detection performance is compared in terms of the average onset detection delay $(\hat{n} - n)$. The root mean square error (RMSE) of the state estimate is used to compare the tracking performance, which is defined as

$$\text{RMSE}(\hat{x}_k) = \sqrt{\frac{1}{N}\sum_{i=1}^{N}(x_k - \hat{x}_k)'(x_k - \hat{x}_k)} \tag{13}$$

where N is the number of Monte Carlo runs; x_k is the true state vector; and $\hat{x}_k$ is the estimated state.

5.2.2. Measure for Filter Credibility

The filter credibility analysis is done by calculating the average normalized estimation error squared (ANEES). Denote by $(x_i - \hat{x}_i)$ the vector of state estimation error in run i; P_i =cov$(x_i - \hat{x}_i)$, N the total number of runs, and $n = \dim(x)$. The ANEES is defined as follows.

$$\psi_{\text{ANEES}} = \frac{1}{Nn}\sum_{i=1}^{N}(x_i - \hat{x}_i)' P_i^{-1}(x_i - \hat{x}_i) \tag{14}$$

The closer the ANEES is to 1, the more credible the filter is.

5.3. Simulation Results

All results are averages over 100 Monte Carlo runs. The tracking period begins at 100 sec after time zero and continues for 150 sec in the first two scenarios and 200 sec for the last scenario. This ensures a fair comparison by letting initial errors stabilize and all trackers have the same starting point at the end of the startup period. The threshold for each detector was determined by simulations under scenario E2C0 with a given false alarm rate $P_{fa} = 1\%$. Model transition probability matrix used in the IMM is $P = \begin{bmatrix} 0.9 & 0.1 \\ 0.1 & 0.9 \end{bmatrix}$.

5.3.1. Filter Design

To make filters credible, we should properly design process and measurement noise covariances Q and R, respectively. The process noise covariance for the WNA model is given by $Q = q \cdot \begin{bmatrix} Q_1 & O \\ O & Q_1 \end{bmatrix}$, where $Q_1 = \begin{bmatrix} \frac{1}{3}T^3 & \frac{1}{2}T^2 \\ \frac{1}{2}T^2 & T \end{bmatrix}$, $O = \begin{bmatrix} 0 & 0 \\ 0 & 0 \end{bmatrix}$, and T is the sampling interval. Therefore, the key is to choose the value of q.

In the simulations, we found that q in the filter using range rate measurements should be larger than the one without $\dot{r}$ in order to keep filter credible in terms of ANEES. However, such a filter is pessimistic in terms of normalized innovation squared (NIS). A possible reason may come from the errors caused by linearization in the measurement model where range rate measurements are actually highly nonlinear in states. The $c_{\min 2}$ filter needs a different design in terms of credibility since it does not use range rate measurements in state estimation update. Table 1 lists the corresponding noise covariances used in WNA-L and WNA-H models of the E2C scenarios for different trackers. $R = (11)^2 I$ was used for all tested E2C scenarios based on the true range standard deviation. More detailed discussions about filter design can be found elsewhere.[23]

Table 1. Filter design of process noise PSD q in the unit of $\mathrm{m}^2/\mathrm{s}^3$

q	WNA-L, Q_{low}	WNA-H, Q_{high}
detectors without rdot	10	500
detectors with rdot	30	2000
$c_{\min 3}$	0.8	800
IMM	5	1000

5.3.2. Approximate Distributions for Generalized Page's Test

The approximate Gamma distributions for tangential and normal accelerations were obtained for small maneuver magnitude. Fig. 1 and Fig. 2 show the histogram and the approximate Gamma distribution for two scenarios E2C0 and E2C(a_n,20). We can see that these empirical distributions are uni-modal but with peaks larger than the true maneuver magnitude. More simulation results not listed here show that the distribution of $c_{\min 2}$ depends on the accuracy of the range rate measurement, target motion types and target geometry.[23]

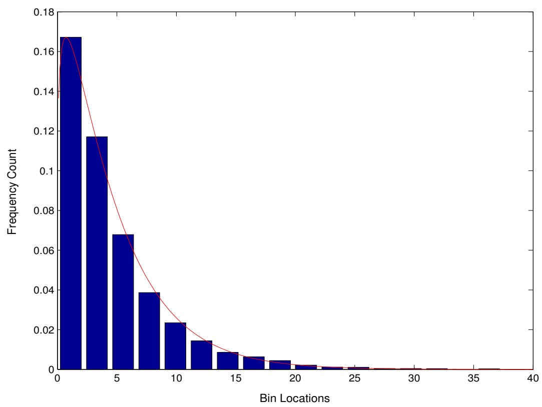

Figure 1. Bar plot vs. Gamma pdf: non-maneuver

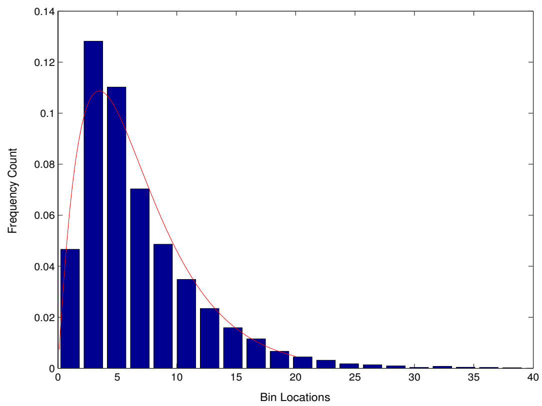

Figure 2. Bar plot vs. Gamma pdf: E2C(a_n,20)

5.3.3. Comparison of Detection Performance

The detection performance of different detectors is compared over different E2C scenarios under a given false alarm rate $P_{fa} = 1\%$. Here MR and MR(noRate) denote the measurement residual based detectors with and without range rate measurements, respectively. The window size used by MR based detectors is 5. We denote $c_{\min}$ and $c_{\min 2}$ the maneuver detectors based on statistics $c_{\min}$ and $c_{\min 2}$, respectively. Denote by $c_{\min 2\_\mathrm{CUSUM}}$ Page's detector based on $c_{\min 2}$ with the approximate Gamma distribution. Denote by $c_{\min 3\_\mathrm{CUSUM}}$ Page's detector based on $c_{\min 3}$ that uses range rate measurement only for detection but not for update state estimate. Detailed simulation setup and parameter settings can be found elsewhere.[23] The average onset detection delays for different detectors are listed in Table 2.

Table 2. Average detection delay of maneuver onset time ($P_{fa} = 1\%$)

$\hat{n} - n$	E2C(a_t,10)	E2C(a_t,20)	E2C(a_n,20)	E2C(a_n,30)
MR(noRate)	17.05	10.65	39.58	29.56
MR	35.37	5.74	44.22	34.42
$c_{\min}$	1.70	1.00	22.12	14.86
$c_{\min 2}$	1.54	1.00	23.4	12.99
$c_{\min 2\_\mathrm{CUSUM}}$	1.54	0.99	26.82	19.01
$c_{\min 3\_\mathrm{CUSUM}}$	1.59	1.01	3.74	2.64

Table 2 shows that using range rate measurements does improve the detection performance for all tested scenarios. The $c_{\min 3\_\mathrm{CUSUM}}$ detector almost always has the best performance for all scenarios. The performance of the $c_{\min 2\_\mathrm{CUSUM}}$ detector depends on the accuracy of the approximate Gamma distribution of the total acceleration. The $c_{\min 2\_\mathrm{CUSUM}}$ and $c_{\min 2}$ detectors had comparable performance.

5.3.4. Comparison of Estimation Performance

In this section, the tracking performance is compared under scenarios E2C(a_n, 30) and E2C(a_n,20)-E2C(a_t,20). Fig. 3 and Fig. 4 shows the position and velocity RMSE for the two scenarios, respectively. Denote by MR(ideal) the tracker with the process noise level changing from Q_{low} to Q_{high} at the exact maneuver onset time with the range rate measurements. This estimator provides a baseline solution for comparison.

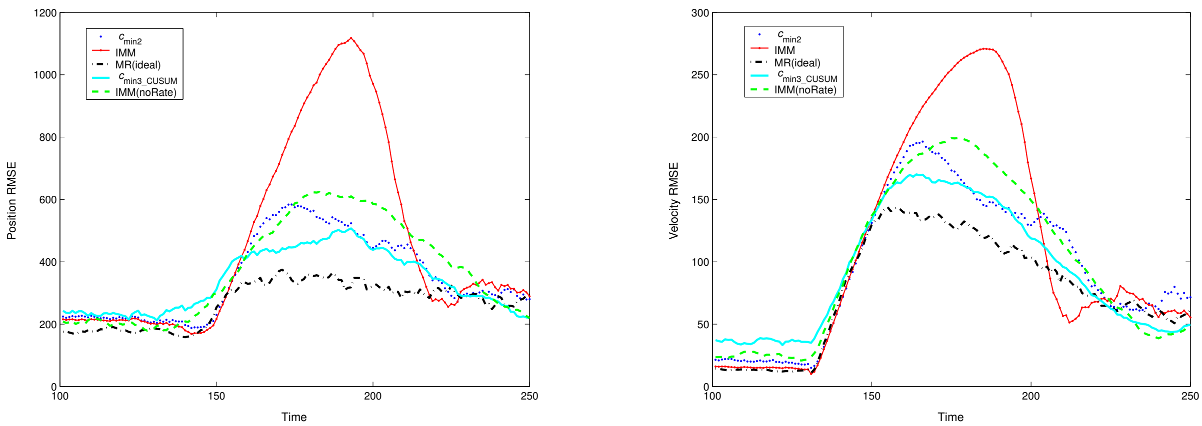

Figure 3. RMSE of scenario E2C(a_n,30)

It can be seen that the tracking accuracy based on the $c_{\min 3\_\mathrm{CUSUM}}$ detector improved in both position and velocity components after the target maneuvers, which outperforms other trackers including the IMM tracker and is closest to the ideal MR based tracker. In terms of credibility of the ANEES shown in Fig. 5 (left: $c_{\min 3\_\mathrm{CUSUM}}$, right: IMM), both $c_{\min 3\_\mathrm{CUSUM}}$ and IMM trackers are pessimistic during non-maneuver segment and optimistic during maneuver segment compared with the 95% confidence interval of the ANEES. The $c_{\min 3\_\mathrm{CUSUM}}$ tracker is more credible than IMM tracker during target maneuver. In this scenario, the performance of the IMM tracker could not be improved more even with different filter designs. Due to slow detection, the IMM has a large overshoot which is inline with the MR because the IMM model switching is actually based on measurement

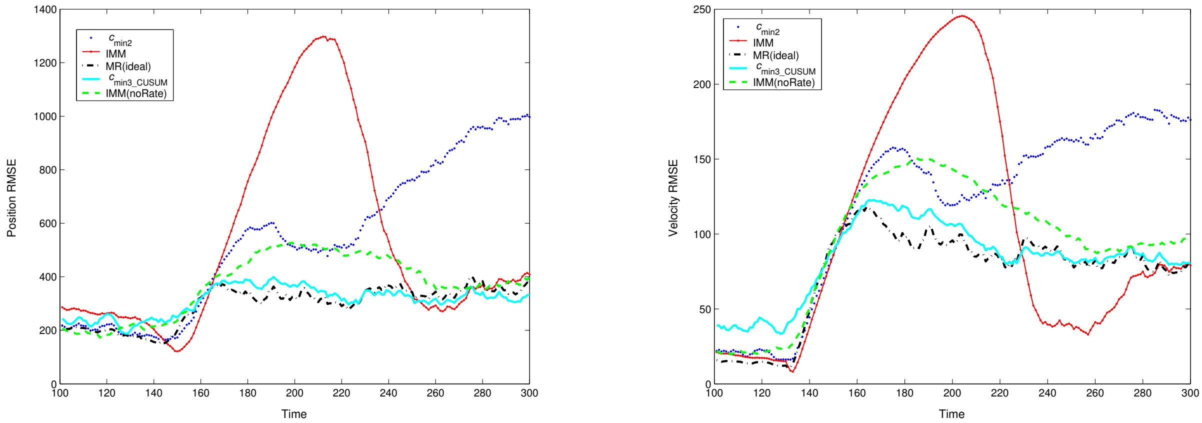

Figure 4. RMSE of scenario E2C(a_n,20)-E2C(a_t,20)

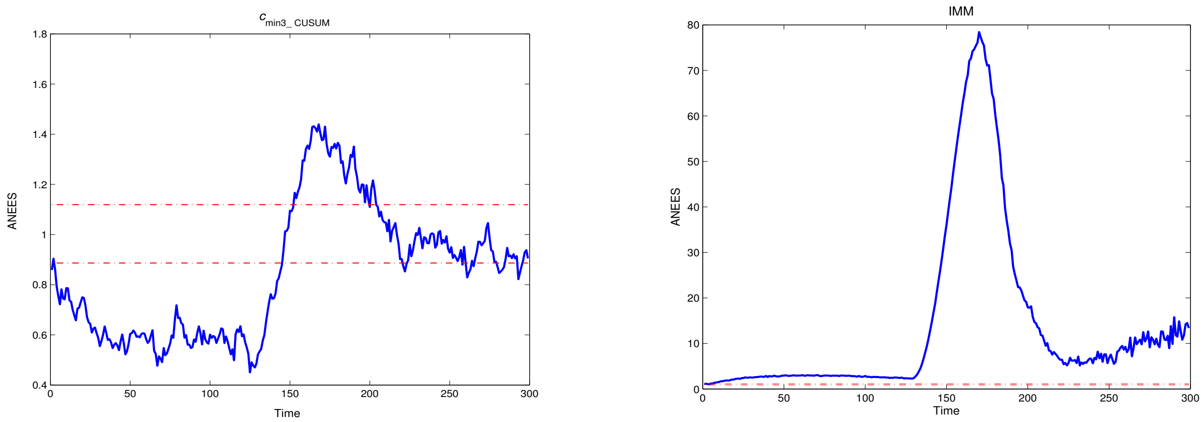

Figure 5. ANEES of scenario E2C(a_n,20)-E2C(a_t,20)

residuals. It is hard for the $c_{\min 2}$ tracker to detect the second maneuver in E2C(a_n,20)-E2C(a_t,20), which increased estimation errors. This is because that the test statistics of normal and tangential accelerations based on $c_{\min 2}$ have different distributions, which makes it difficult to detect by a single threshold.

6. PERFORMANCE COMPARISON USING STEADY STATE ANALYSIS

In this section, we want to quantitatively study the performance improvement using range rate measurements in terms of the estimation error covariance in the steady state. To make the formulation analytically tractable and the results meaningful as a guidance for filter design, we assume the tracker is implemented in a radar local coordinate system with x and y axes along the range and cross range. Thus the range rate measurement will only affect the tracking accuracy along the line of sight. Without loss of generality, we consider the one dimensional target motion with the state vector given by $\mathbf{x}_k = [x_k, \dot{x}_k]'$. The target dynamics and the two observation models with and without range rate measurements are

$$\begin{aligned} \mathbf{x}_k &= F_2 \mathbf{x}_{k-1} + G_2 w_k \\ z_{1c}(k) &= \begin{bmatrix} 1 & 0 \end{bmatrix} \mathbf{x}_k + v_{1k} \triangleq H_1 \mathbf{x}_k + v_{1k} \\ z_{2c}(k) &= I_{2\times 2} \mathbf{x}_k + v_{2k} \triangleq H_2 \mathbf{x}_k + v_{2k} \end{aligned}$$

where $H_1 = \begin{bmatrix} 1 & 0 \end{bmatrix}$, $H_2 = I_{2\times 2}$, $w_k \sim N(0, \sigma_w^2)$, $v_{1k} \sim N(0, \sigma_v^2)$ and $v_{1k} \sim N(0, R_2)$. We assume that $R_2 = \begin{bmatrix} \sigma_v^2 & 0 \\ 0 & \sigma_{\dot{v}}^2 \end{bmatrix}$.

The steady state Kalman filter for observation with and without range rate are given by[4]

$$\hat{x}_{1c}(k+1) = F\hat{x}_{1c}(k) + FK_1[z_{1c}(k) - H_1\hat{x}_{1c}(k)]$$
$$\hat{x}_{2c}(k+1) = F\hat{x}_{2c}(k) + FK_2[z_{2c}(k) - H_2\hat{x}_{2c}(k)] = F\hat{x}_{2c}(k) + FK_2[z_{2c}(k) - \hat{x}_{2c}(k)]$$

where $\hat{x}_{1c}(k)$ and $\hat{x}_{2c}(k)$ are state estimates, and the Kalman filter gain K_1 and K_2 are given by

$$K_1 = P_1H_1'(H_1'P_1H_1 + \sigma_v^2)^{-1}$$
$$K_2 = P_2H_2'(H_2'P_2H_2 + R_2)^{-1} = P_2(P_2 + R_2)^{-1}$$

Note that P_1 and P_2 are the steady state a priori error covariance matrices with or without the range rate information. They are the solutions to the following algebraic Racatti equations

$$P_1 = F[P_1 - P_1H_1'(H_1P_1H_1' + \sigma_v^2)^{-1}H_1P_1]F' + \sigma_w^2GG' \tag{15}$$

$$P_2 = F[P_2 - P_2(P_2 + R_2)^{-1}P_2]F' + \sigma_w^2GG' \tag{16}$$

For the discrete time white noise acceleration model, there exists the analytical solution for $p_{11}^{(1)}$, $p_{12}^{(1)}$ and $p_{22}^{(1)}$ given by[4]

$$P_1 = \begin{bmatrix} p_{11}^{(1)} & p_{12}^{(1)} \\ p_{21}^{(1)} & p_{22}^{(1)} \end{bmatrix} = \begin{bmatrix} \alpha & \frac{\beta}{T} \\ \frac{\beta}{T} & \frac{\beta(\alpha-\beta/2)}{(1-\alpha)T^2} \end{bmatrix} \sigma_v^2 \tag{17}$$

where $\alpha = \frac{1}{8}(\lambda^2 + 8\lambda - (\lambda+4)\sqrt{\lambda^2+8\lambda})$, $\beta = \frac{1}{4}(\lambda^2 + 4\lambda - \lambda\sqrt{\lambda^2+8\lambda})$ and the target maneuvering index is defined as $\lambda = \frac{\sigma_w T^2}{\sigma_v}$.

Fig. 6–Fig. 7 show the steady state filter gain for the cases with and without range rate measurements. We can see that the steady state filter gain with range rate measurement is very different from the α-β filter and its analytical expression is much more involved than (17).

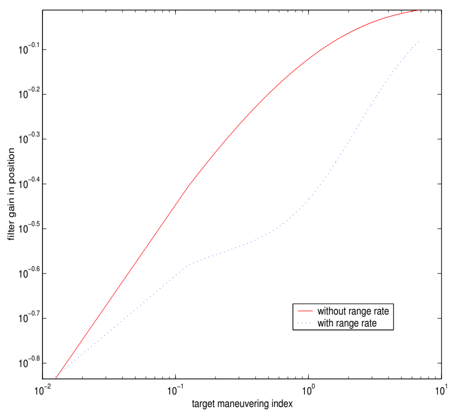

Figure 6. Steady state filter gain of position component: with range rate vs. without range rate

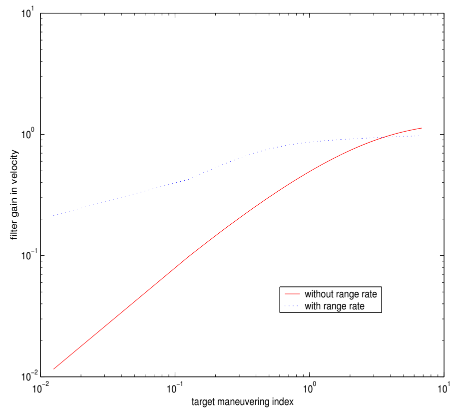

Figure 7. Steady state filter gain of velocity component: with range rate vs. without range rate

Fig. 8–Fig. 9 show the estimation error variances in position and velocity for various target maneuvering indices compared with the ideal bound given by the covariance of the process noise. We can see that in the steady state, both filters approach the ideal error bound. The filter with range rate measurement has a saturation region for position estimation error variance for the target maneuvering index below 0.2. Similar characteristics can be seen from Fig. 9 where the velocity estimation error variance approaches the ideal error bound when the range rate measurement is available. Clearly, the benefit of using range rate measurements for the improvement of estimation accuracy lies in a certain range of the target maneuver index. When the target maneuvering index is very small, the target motion model is fairly accurate and the improvement through range rate measurements

is small. Alternatively, when the target maneuvering index is very large, the target motion uncertainty can not be significantly reduced using the range rate measurements. The analysis, although quite simplified with the white noise acceleration model, reveals that there exists a certain range of practical interest, e.g., target maneuvering index within (0.05, 1), that the filter using range rate measurements can improve the estimation accuracy significantly. This also explains the simulation results, where tracking accuracy improves more in velocity than in position for various target maneuver motions with a moderate magnitude.

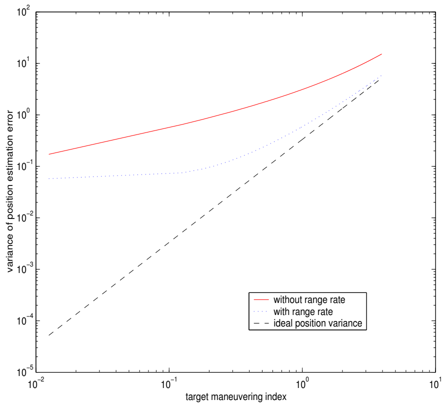

Figure 8. Position estimation error variances: with range rate, without range rate, and ideal case

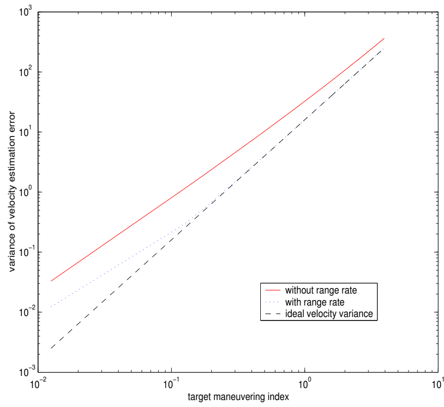

Figure 9. Velocity estimation error variances: with range rate, without range rate, and ideal case

7. CONCLUSIONS AND FUTURE WORK

In this paper, we studied the maneuver detection using Page's test based on the estimated total acceleration. In addition, a simple measurement conversion technique is used to treat range rate as a linear measurement so that a Kalman filter can be applied. Extensive simulation comparison in terms of detection and tracking has been carried out under different E2C scenarios. The performance improvement in terms of tracking accuracy is observed for both tangential and normal accelerations compared with the popularly used IMM tracker. The ideal performance limit using range rate measurements is also quantified through a steady state analysis with a simplified filter model under various target maneuvering indices. The plots indicate the existence of a region of target motion uncertainty where the tracking accuracy improves significantly in both position and velocity estimates.

Future work may include the following: Investigate the filter design issue, especially for tracking based on the detection of the generalized Page's test when true maneuvers are unknown. Explore the potential of using range rate statistic for model set design when the target maneuver type and magnitude are unknown. Further develop non-simulation based performance prediction using steady state analysis to quantify the benefit of using range rate measurements when the target-senor geometry is also included in the formulation. It has important implication to the use of multi-sensor data fusion to enhance the tracking performance.

8. ACKNOWLEDGEMENT

This research work is supported in part by ARO grants W911NF-04-1-0274 and W911NF-05-1-0107, NSF/LEQSF-Pfund-38, NAVY SBIR N68335-05-C0028, and NASA/LEQSF grant (2001-4)-01.

Appendix A. Range Rate Measurement Conversion for Kalman Filter

Here we present a measurement conversion technique when the range rate is treated as a linear measurement for the Kalman filtering. For convenience, the time index is dropped in the measurement equation. Denote the converted measurement from the polar ($r_m = r + w_r$, $\theta_m = \theta + w_\theta$, $\dot{r}_m = \dot{r} + w_{\dot{r}}$) to the Cartesian coordinates as $z^m = [\begin{array}{ccc} x_m & y_m & \dot{r}_m \end{array}]'$, where r, θ and $\dot{r}$ are the true range, bearing and range rate, respectively; $w_r \sim \mathcal{N}(0, \sigma_r^2)$,

$w_\theta \sim \mathcal{N}(0, \sigma_\theta^2)$ and $w_\theta \sim \mathcal{N}(0, \sigma_{\dot{r}}^2)$ are independent measurement noise. The unbiased measurement conversion of the position measurement in the Cartesian coordinates is[3]

$$x_m = b_1^{-1} r_m \cos\theta_m \tag{18}$$

$$y_m = b_1^{-1} r_m \sin\theta_m \tag{19}$$

where $b_1 \triangleq E[\cos w_\theta] = e^{-\sigma_\theta^2/2}$ is the multiplicative bias introduced by the measurement conversion. Denote by $b_2 \triangleq E[\cos 2w_\theta] = e^{-2\sigma_\theta^2}$. The corresponding covariances of the converted position measurement R_{11}, R_{22}, R_{12} can be calculated conditioning on the position observations $(r_m,\, \theta_m)$.[3]

Assuming the measured target bearing is accurate enough, according to the target dynamics $\dot{r} = \dot{x}\cos\theta + \dot{y}\sin\theta$, by replacing the true target bearing with the measured one, we have the linear measurement equation including the range rate given below

$$z_k^m = \begin{bmatrix} 1 & 0 & 0 & 0 \\ 0 & 0 & 1 & 0 \\ 0 & b_1^{-1}\cos\theta_k^m & 0 & b_1^{-1}\sin\theta_k^m \end{bmatrix} x_k + v_k \tag{20}$$

To obtain the corresponding covariance, the squared error should be averaged conditioned on the observations $(r_m,\, \theta_m)$. After some algebraic manipulation, we have

$$\begin{aligned} R_{13} &\triangleq \mathrm{cov}(x_m, \dot{r}_m) = E[(b_1^{-1} r_m \cos\theta_m - r\cos\theta)(b_1^{-1}(\dot{x}\cos\theta_m + \dot{y}\sin\theta_m) - \dot{x}\cos\theta + \dot{y}\sin\theta) | r_m, \theta_m] \\ &= \frac{b_1^{-2} + b_2 - 2}{2} r_m(\dot{y}\sin 2\theta_m + \dot{x}\cos 2\theta_m) + \frac{b_1^{-2} - 1}{2} r_m \dot{x} \end{aligned} \tag{21}$$

$$\begin{aligned} R_{23} &\triangleq \mathrm{cov}(y_m, \dot{r}_m) = E[(b_1^{-1} r_m \sin\theta_m - r\sin\theta)(b_1^{-1}(\dot{x}\cos\theta_m + \dot{y}\sin\theta_m) - \dot{x}\cos\theta + \dot{y}\sin\theta) | r_m, \theta_m] \\ &= \frac{b_1^{-2} + b_2 - 2}{2} r_m(\dot{x}\sin 2\theta_m - \dot{y}\cos 2\theta_m) + \frac{b_1^{-2} - 1}{2} r_m \dot{y} \end{aligned} \tag{22}$$

$$\begin{aligned} R_{33} &\triangleq \mathrm{cov}(\dot{r}_m, \dot{r}_m) = E[(b_1^{-1}(\dot{x}\cos\theta_m + \dot{y}\sin\theta_m) - \dot{x}\cos\theta + \dot{y}\sin\theta)^2 | r_m, \theta_m] \\ &= \left[(b_1^{-2} - 2)\cos^2\theta_m + \frac{1 + b_2\cos 2\theta_m}{2}\right]\dot{x}^2 + \left[(b_1^{-2} - 2)\sin^2\theta_m + \frac{1 - b_2\cos 2\theta_m}{2}\right]\dot{y}^2 \\ &+ (b_1^{-2} + b_2 - 2)\dot{x}\dot{y}\sin 2\theta_m + \sigma_{\dot{r}}^2 \end{aligned} \tag{23}$$

and R_{11}, R_{12}, R_{22} were derived in.[3] Since the true $\dot{x}_k$ and $\dot{y}_k$ are not available in practice, we use the state estimate from time $k-1$ instead, i.e., $\hat{x}_{k-1|k-1}$ and $\hat{y}_{k-1|k-1}$.

REFERENCES

1. Y. Bar-Shalom and H. Chen. IMM Estimator with Out-of-Sequence Measurements. *IEEE Trans. Aerospace and Electronic Systems*, 41(1):90–98, Jan. 2005.
2. Y. Bar-Shalom and X. R. Li. *Estimation and Tracking: Principles, Techniques, and Software.* Artech House, Boston, MA, 1993. (Reprinted by YBS Publishing, 1998).
3. Y. Bar-Shalom and X. R. Li. *Multitarget-Multisensor Tracking: Principles and Techniques.* YBS Publishing, Storrs, CT, 1995.
4. Y. Bar-Shalom, X. R. Li, and T. Kirubarajan. *Estimation with Applications to Tracking and Navigation: Theory, Algorithms, and Software.* Wiley, New York, 2001.
5. M. Basseville and I. Nikiforov. *Detection of Abrupt Changes: Theory and Application.* Prentice Hall, Englewood Cliffs, NJ, 1993.
6. D. F. Bizup and D. B. Brown. Maneuver Detection Using the Range Rate Measurement. *IEEE Trans. Aerospace and Electronic Systems*, AES-40(1):330–336, Jan. 2004.
7. S. S. Blackman and R. F. Popoli. *Design and Analysis of Modern Tracking Systems.* Artech House, Norwood, MA, 1999.

8. Y. P. Dai, C. Z. Jin, J. L. Hu, K. Hirasawa, and Z. Liu. Target Tracking under Dense Environment Using Range Rate Measurements. In *Proc. 38th SICE (Society of Instrument and Control Engineers) Annual Conference*, pages 1145–1148. SICE, 1999.
9. Z.-S. Duan, C.-Z. Han, and X. R. Li. Radar Target Tracking with Range Rate Measurements in Spherical Coordinates. In *Proc. 2004 International Conf. on Information Fusion*, pages 599–605, Stockholm, Sweden, June-July 2004.
10. Z.-S. Duan, C.-Z. Han, and X. R. Li. Sequential Unscented Kalman Filter for Radar Target Tracking with Range Rate Measurements. In *Proc. 2005 International Conf. on Information Fusion*, pages A4–4, Philadelphia, PA, July 2005.
11. A. Farina and F. A. Studer. *Radar Data Processing, vol. I: Introduction and Tracking, vol. II: Advanced Topics and Applications*. Research Studies Press, Letchworth, Hertfordshire, England, 1985.
12. H. Kameda, S. Tsujimichi, and Y. Kosuge. Target Tracking under Dense Environment Using Range Rate Measurements. In *Proc. 37th SICE (Society of Instrument and Control Engineers) Annual Conference*, pages 927–932. SICE, 1997.
13. T. L. Lai. Sequential Multiple Hypothesis Testing and Efficient Fault Detection-Isolation in Stochastic Systems. *IEEE Trans. on Information Theory*, 46(2):595–608, Mar. 2000.
14. T. L. Lai and J. Z. Shan. Efficient Recursive Algorithms for Detection of Abrupt Changes in Signals and Controls Systems. *IEEE Trans. on Automatic Control*, 44(5):952–966, May 1999.
15. X. R. Li. Model-Set Design for Multiple-Model Estimation—Part I. In *Proc. 2002 International Conf. on Information Fusion*, pages 26–33, Annapolis, MD, USA, July 2002.
16. X. R. Li and V. P. Jilkov. A Survey of Maneuvering Target Tracking—Part III: Measurement Models. In *Proc. 2001 SPIE Conf. on Signal and Data Processing of Small Targets,* vol. 4473, pages 423–446, San Diego, CA, USA, July-Aug. 2001.
17. X. R. Li and V. P. Jilkov. A Survey of Maneuvering Target Tracking—Part IV: Decision-Based Methods. In *Proc. 2002 SPIE Conf. on Signal and Data Processing of Small Targets,* vol. 4728, Orlando, Florida, USA, April 2002.
18. X. R. Li and V. P. Jilkov. Survey of Maneuvering Target Tracking—Part I: Dynamic Models. *IEEE Trans. Aerospace and Electronic Systems*, AES-39(4), Oct. 2003.
19. X. R. Li and V. P. Jilkov. A Survey of Maneuvering Target Tracking—Part V: Multiple-Model Methods. *IEEE Trans. Aerospace and Electronic Systems*, 42(1), Jan. 2006.
20. X. R. Li, Z.-L. Zhao, P. Zhang, and C. He. Model-Set Design for Multiple-Model Estimation—Part II: Examples. In *Proc. 2002 International Conf. on Information Fusion*, pages 1347–1354, Annapolis, MD, USA, July 2002.
21. I. Nikiforov. Optimal Sequential Change Detection and Isolation. In *Proc. 15th IFAC Word Congress*, Barcelona, Spain, July 2002.
22. J.-F. Ru, A. Bashi, and X. R. Li. Performance Comparison of Target Maneuver Onset Detection Algorithms. In *Proc. 2004 SPIE Conf. on Signal and Data Processing of Small Targets,* vol. 5428, 2004.
23. J.-F. Ru, H. Chen, and G. S. Chen. Maneuvering Target Detection and Tracking using Range Rate Measurements. Technical report, Dept. of Electrical Engineering, University of New Orleans, April. 2005.
24. J.-F. Ru, V. P. Jilkov, X. R. Li, and A. Bashi. Sequential Detection of Target Maneuvers, in Proc. of International Conference on Information Fusion 2005. Philadophia, PA, July 2005.
25. R. Schutz, B. Engelberg, W. Soper, and R. Mcallister. Maneuver Tracking Algorithms for AEW Target Tracking Applications. In *Proc. 1999 SPIE Conf. on Signal and Data Processing of Small Targets,* vol. 3809, 1999.
26. R. Schutz, R. Mcallister, B. Engelberg, V. Maone, R. Helm, V. Kats, C. Dennean, W. Soper, and L. Moran. Combined Kalman Filter (CKF) and JVC algorithms for AEW Target Tracking Applications. In *Proc. 1997 SPIE Conf. on Signal and Data Processing of Small Targets,* vol. 3163, 1997.
27. P. Suchomski. Explicit Expressins for Debiased Statistics of 3D Converted Measurements. *IEEE Trans. Aerospace and Electronic Systems*, AES-35(1):368–370, 1999.
28. S. Zollo and B. Ristic. On Polar and versus Cartesian Coordinates for Target Tracking. In *Proc. The Fifth International Symposium on Signal Processing and its Applications*, pages 499–502, Brisbane, Australia, 1999.